

Spreading behavior of firefighting foam solutions on typical liquid fuel surfaces

Youjie Sheng (✉ youjies@xust.edu.cn)

Xi'an University of Science and Technology

Yang Li

Xi'an University of Science and Technology

Kui Wu

Xi'an University of Science and Technology

Research Article

Keywords: Firefighting foam solution, liquid fuel surface, film-forming, spreading behavior, spreading rate, spreading amount

Posted Date: February 18th, 2021

DOI: <https://doi.org/10.21203/rs.3.rs-208743/v1>

License:  This work is licensed under a Creative Commons Attribution 4.0 International License. [Read Full License](#)

Abstract

A series of experiments was performed to investigate the spreading behavior of firefighting foam solutions on liquid fuel surfaces. The spreading coefficients of six kinds of aqueous film-forming foam solutions and one fluorine-free foam solution on the surface of four liquid fuels, namely, cyclohexane, diesel, n-heptane, and ethanol, were calculated on the basis of surface and interfacial tension. Spreading behavior was studied systematically using a high-speed camera, and then the relationship between spreading behavior and spreading coefficient was analyzed. Furthermore, the spreading area and spreading rate of different foam solution droplets on liquid fuel surfaces were studied in depth. The spreading amount of the foam solution droplets on the liquid fuel surfaces was measured. Four typical spreading phenomena, namely, spreading, suspension, dissolution, and sinking, of AFFF solutions on liquid fuel surfaces were identified. Moreover, a positive spreading coefficient did not necessarily lead to the formation of an aqueous film. The spreading area, spreading rate, and spreading amount were not proportional to the spreading coefficient. During the evaluation of the spreading property of firefighting foam, the spreading coefficient, spreading rate, and spreading amount must be focused on instead of only the spreading coefficient.

1. Introduction

The phenomena of droplet interaction with a surface widely exists in many industrial applications [1–5], such as fire suppression by water spray/mist [6], spray cooling, dissolved oxygen increment, inkjet printing [7], and rain fall calculation [8]. Considerable researches have been focused on the typical phenomena of droplet interaction with hydrophobic surface, such as bouncing, coalescence, injecting and splashing [8–13]. However, most of these researches focused on the impact of droplets with a certain initial momentum on liquid surface. Few studies have been focused on the spreading phenomenon of a liquid droplet with a very low initial momentum on another immiscible liquid surface.

Theoretically, a liquid droplet with a high density can spread on another immiscible liquid surface with a low density. And the occurrence of the spreading phenomenon depends on the spreading coefficient, which is calculated using Eq. (1) [14–16].

$$S = \gamma_o - \gamma_w - \gamma_{ow}, (1)$$

where S is the spreading coefficient, γ_o is the surface tension of the lower liquid, γ_w is the surface tension of the upper liquid, and γ_{ow} is the interfacial tension between the two liquids. The spreading phenomenon of surfactant solution droplet on liquid fuel surface has been widely used in the fire extinguishing agent of aqueous film-forming foam (AFFF) [16–20]. AFFF is considered the most efficient among fire extinguishing agents used to fight liquid fuel fire. Its high effectiveness in fire extinguishment is provided not only by the foam layer but also by an aqueous film layer on the liquid fuel surface upon AFFF application. The spreading coefficient is the only parameter for evaluating the property of the aqueous film layer in most of international standard related to AFFF [21, 22]. For AFFF, the upper liquid is the aqueous solution of AFFF, and the lower liquid is the liquid fuel.

Many properties of traditional AFFFs have been studied to understand the contribution of foam layer to fire suppression; such properties include rheological [23], foam spread [17], foam drainage [24, 25], and fire extinguishing and burn-back performance [26–28]. However, studies that focus on the aqueous film layer generated by the AFFF solution on liquid fuel surfaces are few [19]. The AFFF solution is supposed to be able to spread and form an aqueous film layer on the fuel surface only if $S > 0$ [21, 22]. Some recent studies have shown that some solutions cannot form an aqueous film on the liquid fuel surface even though the spreading coefficient is positive [15, 18, 29, 30]. The emergence of these new issues indicated that the formation regime of aqueous films on liquid fuel surfaces is unclear. In addition, these studies only focused on whether aqueous films formed on the liquid fuel surface or not; only a few focused on film properties, such as the film-forming process and film spreading rate. Therefore, further research on the spreading properties of AFFF solutions should be conducted to enhance our understanding.

To investigate the film-forming property of AFFF solutions on liquid fuel surfaces, the present study conducts a series of experiments on the spreading coefficient of several commercial AFFFs, Alcohol-resist AFFFs (AR-AFFFs), and a fluorine-free firefighting foam on surface of typical liquid fuels. The spreading process, spreading rate, and spreading amount of AFFF

droplets are studied systematically, and the relationship among the spreading coefficient, spreading process, spreading rate and spreading amount is analyzed in depth. This study can provide guidance for a clear understanding of the formation of aqueous films on liquid fuel surfaces.

2. Experimental

2.1 Materials

2.1.1 Liquid fuel

Four liquid fuels, namely, cyclohexane, diesel, n-heptane, and ethanol, were used in this study. Cyclohexane is the standard liquid fuel used to test the film-forming property of firefighting foam solutions in most international firefighting foam standards [21, 22]. Diesel and n-heptane are two typical liquid fuels that are often used to conduct experiments on liquid fuels. Ethanol is a kind of alcohol fuel. Most alcohol fuels are miscible with water and difficult to extinguish upon ignition. The basic properties of the four liquid fuels are listed in Table 1.

Table 1
The basic properties of liquid fuels

Liquid fuel	Density (g/cm ³)	Boiling point (°C)	Surface tension (mN/m)	Viscosity(mPa·s)	Water solubility
Cyclohexane	0.78	80.7	24.17	0.94	Insoluble
Diesel	0.85	180 ~ 370	27.04	4.18	Insoluble
n-heptane	0.68	98.5	19.62	0.41	Insoluble
Ethanol	0.79	78.3	21.83	1.09	Miscible

2.1.2 Firefighting foams

Seven commercial firefighting foam concentrates were used in this study. Three percent AFFF, 3% AR-AFFF, 6% AFFF, 6% AR-AFFF were purchased from Xi'an Yutai Fire Protection Technology Co., Ltd.; for convenience, these concentrates were denoted as AFFF-1#, AFFF-2#, AFFF-3#, and AFFF-4#, respectively. Six percent AFFF (resistant to seawater) was purchased from Danyang Jixingyu Fire Equipment Co. Ltd. and denoted as AFFF-5#. Three percent AFFF (resistant to seawater) was a gift from the fire corps of Shaanxi Province and denoted as AFFF-6#. A kind of fluorine-free foam was obtained from the fire corps of Shaanxi Province and denoted as FfreeF. The firefighting foams with 3% concentration were diluted using fresh water at a volume ratio of 3:97. The foams with 6% concentration were diluted using fresh water at a volume ratio of 6:94. Lastly, the FfreeF foam concentrate was diluted using fresh water at a volume ratio of 1:99.

2.2 Apparatus and methods

The dynamic surface tension governs many important industrial and biological processes [31]. Compared to equilibrium surface tension, the dynamic surface tension better reflects the adsorption behavior of surfactant molecules on air/liquid interfaces. In the present study, the dynamic surface tension was measured using a QBZY-3 fully automatic surface tension meter based on the platinum plate method in a water bath at 20°C. At the process of testing, the platinum plate was moved towards the upper surface of foam solution from the top. The platinum plate stopped moving once it touched the upper surface of foam solution. The surface tension increased gradually from the time when the platinum plate touched the upper surface of foam solution. After a period of time, the surface tension became generally stable, and the corresponding value was the equilibrium surface tension. The interfacial tension was measured using a K100 Kruss fully automatic surface tension meter. The spreading coefficient of the AFFF solutions was calculated in accordance with Eq. (1). The dynamic viscosity of the

foam dispersions was measured using a DV-1 digital viscometer. The conductivity of the foam dispersions was measured using an SG23-B Mettler multi-parameter tester. Each experiment was repeated at least three times.

A schematic of the experimental apparatus for spreading behavior is shown in Fig. 1. A syringe pump was used to generate single liquid droplets of the foam solutions. The droplets are formed at the tip of the syringe and then dropped from the needle under the action of gravity. The advancing velocity of foam solution in the syringe pump was 10ul/min, and the droplet diameter was set at a fixed value of approximately 2.6 mm in all experiments. It takes approximate 55s to create a droplet with diameter = 2.6mm before droplet dropped from the needle under the action of gravity. A high-speed digital camera was used to record the spreading process of the foam solution on the liquid fuel surface. A 1,000 W iodine–tungsten light was used as a strong illuminant together with a thin sheet of paper as a diffuser. The liquid fuel with a depth of 20 mm was placed into a square transparent quartz glass container under room temperature. The distance between the liquid fuel surface and the tip of the needle was 5 mm to reduce the impact of the droplet on the fuel surface. The images of spreading process were processed using ImageJ software.

3. Results And Discussion

3.1 Foam solution properties

Figure 2 displays the curves of the dynamic surface tension of the seven firefighting foam solutions. All the foam solutions reached their equilibrium surface tension rapidly, within 10s. This should be ascribed to the high concentration of surfactants in firefighting foam solutions, which is much higher than their critical micelle concentration (cmc). The dynamic surface tension of solutions AFFF-2#, AFFF-6#, and FfreeF increased gradually over time until the equilibrium surface tension was reached. The equilibrium surface tensions of the three solutions were 16.09 mN/m at 4.4 s, 17.41 mN/m at 5 s, and 24.68 mN/m at 5.7 s, respectively. The surface tensions of AFFF-1#, AFFF-3#, AFFF-4# and AFFF-5# increased rapidly and reached the maximum value, and then dropped to their equilibrium surface tension which were 17.28mN/m at 6.5s, 20.45 mN/m at 10 s, 16.21 mN/m at 10 s, and 18.66 mN/m at 3.6 s, respectively. Obviously, AFFF-5# has the strongest ability to reach adsorption equilibrium. The equilibrium surface tensions of the solutions are lower than 25 mN/m, whereas those AFFF solutions except AFFF-3# and FfreeF are even lower than 20 mN/m, indicating that all the foam solutions have a high surface activity.

The data of the interfacial tension between foam solutions and liquid fuels, spreading coefficient, dynamic viscosity, and conductivity were listed in Table 2. Notably, the interface between ethanol and foam solution is nonexistent due to the good intermiscibility of ethanol with foam solution. Thus, no data of interfacial tension between ethanol and foam solution and corresponding spreading coefficient was shown in Table 2.

Table 2
Foam solution properties

Samples	Surface tension (mN/m)	Interfacial tension (mN/m)			Spreading coefficient			Viscosity (mPa·s)	Conductivity (mS/cm)
		Diesel	Cyclohexane	n-heptane	Diesel	Cyclohexane	n-heptane		
AFFF-1#	17.28	0.94	1.35	2.33	8.82	5.54	0.01	0.99	2.18
AFFF-2#	16.09	0.79	0.82	1.96	10.16	7.26	1.57	2.66	5.97
AFFF-3#	20.45	0.69	0.52	2.56	5.9	3.2	-3.39	1.86	0.445
AFFF-4#	16.2	0.74	1.19	2.62	10.1	6.78	0.8	3.37	12.2
AFFF-5#	18.66	0.83	1.34	2.52	7.55	4.17	-1.56	2.11	12.32
AFFF-6#	17.41	0.65	0.87	1.62	8.98	5.89	0.59	1.09	0.736
FfreeF	24.68	3.54	1.36	4.13	-1.18	-1.87	-9.19	1.29	0.429

The interfacial tensions between the seven firefighting foam solutions and three liquid fuels show a remarkable difference. The interfacial tensions between the foam solutions and n-heptane are greater than that between the foam solutions and diesel or cyclohexane. AFFF-1#, AFFF-2#, AFFF-4#, AFFF-5#, and AFFF-6# show the lower interfacial tension on the cyclohexane surface than on the diesel surface, whereas AFFF-3# and FfreeF show the lower interfacial tension on the diesel surface than on the cyclohexane surface. The interfacial tension between AFFF-3# and cyclohexane exhibits the minimum value of 0.52 mN/m. The interfacial tension between FfreeF and n-heptane shows the maximum value of 4.13 mN/m.

The spreading coefficients of the seven foam solutions on the diesel and cyclohexane surfaces are positive. In addition, the spreading coefficients of the foam solutions on the diesel surface is greater than that of the cyclohexane surface. The spreading coefficients of AFFF-1#, AFFF-2#, AFFF-4#, and AFFF-6# on the n-heptane surface are positive, but those of AFFF-3#, AFFF-5#, and FfreeF on the n-heptane surface are negative. This result is attributed to the high interfacial tension between the foam solution and n-heptane and the low surface tension of n-heptane.

Big difference existed in the viscosity and conductivity of the foam solutions. The viscosity and conductivity of AFFF-2#, AFFF-4#, and AFFF-5# solutions were obviously higher than other solutions. The differences resulted from the different components of the seven firefighting foams. The firefighting foam usually consisted of hydrocarbon surfactants, fluorocarbon surfactants and foam stabilizers. The high conductivity of AFFF-2#, AFFF-4#, and AFFF-5# solutions means that more ionic surfactants were used. The high viscosity indicated that surfactant or foam stabilizers with high molecular weight were used in foam formulations.

3.2 Spreading dynamics of the foam solutions on liquid fuel surfaces

3.2.1 Typical spreading process

Taking the case of the AFFF-1# solution on the diesel surface as an example, Fig. 3 shows the typical spreading behavior of a single foam solution droplet on a liquid fuel surface. Figure 3(A) and 3(B) show the spreading behavior of the AFFF-1# solution on the diesel surface viewed from the top and viewed from the side, respectively. It should be pointed out that most foam solutions exhibit a spreading behavior similar to that of AFFF-1# on the diesel surface.

The typical process viewed from top can be divided into three stages. In the first stage, the foam solution droplet is released from the syringe pump and touches the liquid fuel surface at 0s. As time passes, the droplet impacts the liquid fuel surface and creates ripples on the surface, as shown in Fig. 3(A) (from 0 ms to 31 ms). In the second stage, the droplet bounces back from the surface due to buoyancy and then drops back to calm after floating on the surface for a certain period. In the third stage, the suspended droplet spreads suddenly and creates ripples on the surface again. At 170 ms, the droplet spreads gradually on the surface, and the spreading area on the liquid fuel surface increases over time. After 25,000 ms, the spreading area comes close to the maximum value, and no evident increase is observed.

The typical process viewed from side showed three stages corresponding to typical process viewed from top. A crater formed and increased over time due to the impact of the foam solution droplet. Then, the crater diminishes gradually after 17 ms, resulting from the spreading of the droplet floating on the fuel surface. All the experiments in which a single droplet can spread on the liquid fuel surface exhibit the same phenomenon as that in Fig. 3(B).

3.2.2 Special spreading process

In addition to the typical spreading behavior, several special spreading behavior are observed, as shown in Fig. 4, Fig. 5, and Fig. 6. The spreading of all the foam solutions on the ethanol surface exhibits a behavior similar to that of AFFF-1#, as described in Fig. 4(A). The foam solution droplet impacts the ethanol surface upon release from the syringe pump, creates ripples on the liquid fuel surface, and then bounces back at 30 ms. A bubble occurs on the surface when the droplet bounces back from the ethanol surface, which is mainly related to the droplet's impact velocity [6, 32–34]. Moreover, the droplet that bounced back is nonspherical. The nonspherical droplet is generated due to the intermiscibility of the foam solution with

ethanol. The droplet does not float on the liquid fuel surface but melts into ethanol in a dispersed manner. At 160 ms, the boundary of the diffusion of foam solution into ethanol looks like a circle. The foam solution droplet is completely dissolved in ethanol after 200 ms, as shown in Fig. 4(A).

Figure 4(B) shows the spreading process of AFFF-1# on the ethanol surface as observed from the side. The process is different from the spreading phenomenon of AFFF-1# on the diesel surface. A crater occurs after the droplet impacts the surface. The droplet does not bounce back but directly sinks to the bottom. The droplet is irregularly shaped while sinking due to the miscibility of ethanol with the foam solution. The foam solution droplet is gradually dissolved into water while sinking, resulting in its irregular shape. The droplet is completely dissolved into ethanol after 200 ms. For the spreading on ethanol surface, all the droplets show a similar spreading behavior as that described in Fig. 4.

The spreading process of AFFF-1# on the n-heptane surface shows another special phenomenon, as illustrated in Fig. 5(A). In the first and second stages, the spreading of AFFF-1# on the n-heptane surface shows a phenomenon similar to the typical spreading process; that is, the single droplet of foam solution impacts the n-heptane surface and then floats on the surface after it bounces back. However, no spreading phenomenon is observed over time. The droplet is suspended on the n-heptane surface, and its spreading area remains unchanged. After 1000 ms, droplet separation occurs. A part of the droplet sinks to the bottom of n-heptane, and the rest of remains suspended on the n-heptane surface. The droplet does not spread completely. The separation of the droplet is mainly attributed to gravity and the limited spreading amount. The spreading behavior of AFFF-2#, AFFF-4#, AFFF-5#, and AFFF-6# on the n-heptane surface are all similar to that of AFFF-1#.

The spreading phenomenon of the AFFF-1# droplet on the heptane surface is shown in Fig. 5(B). The droplet neither sinks immediately nor spreads after impacting the fuel surface. It floats on the fuel surface, and the size of the crater created by the droplet increases gradually over time. After 1,000 ms, the droplet penetrates the fuel surface and breaks away. However, a part of the droplet remains on the surface.

Figure 6(A) shows the spreading behavior of the AFFF-3# droplet on the cyclohexane surface. The spreading process has the same first and second stages as that of the typical spreading phenomenon. The AFFF-3# droplet is bounced back after impacting the cyclohexane surface. Then, the droplet directly sinks to the bottom of cyclohexane, and no spreading or suspension is observed. A bubble-like, spherical, small droplet is generated and floats on the cyclohexane surface even after the droplet has sunk to the bottom. The spreading behavior of the AFFF-3# droplet on the n-heptane surface and that of the FfreeF droplet on all the four liquid fuel surfaces are all similar to that of AFFF-3# on the cyclohexane surface.

The spreading of the AFFF-3# droplet on the cyclohexane surface exhibits a different phenomenon, as illustrated in Fig. 6(B). At 7 ms, a big crater is created by the droplet, but the size of the crater is evidently smaller at 43 ms, indicating that the droplet bounces back from the surface after impacting the cyclohexane surface. At 215 ms, the droplet sinks directly after penetrating the cyclohexane surface, suggesting that the AFFF-3# droplet cannot spread on the cyclohexane surface.

The above results demonstrate that the foam solutions with a negative spreading coefficient do not generate an aqueous film on liquid fuel surfaces; however, a positive spreading coefficient does not necessarily lead to the formation of an aqueous film. Similar results have been observed in some previous studies [15, 18, 30, 35]. Hetzer et al. [30] observed that a positive spreading coefficient ($S > 0$) is necessary but not enough for water film formation. Svitova et al. [35] suggested that this phenomenon was due to the nonequilibrium surface tension effect in the aqueous layer. Fast spreading of surfactant solutions on a liquid fuel surface occurred in the cases when both equilibrium surface tension and dynamic spreading coefficient values were positive. The dynamic spreading coefficient, calculated by use of the dynamic surface tension and dynamic interfacial tension, is the decisive factor for fast spreading. But the real dynamic spreading coefficient cannot be obtained by use of existing technology, because the surface tension and interfacial tension are dynamically changing during droplets interaction with liquid fuel surface. As for the suspension of the AFFF solution droplets on liquid fuel surface, the occurrence of the phenomenon mainly depends on the wettability of liquid fuel surface and droplet's viscosity [36]. The stability of the suspension droplet depends on the combination of three interface tensions, oil density, droplet volume, and the equilibrium contact angle [37].

3.3 Spreading rate of foam solutions on liquid fuel surfaces

3.3.1 Calculation of spreading rate

In this study, a single droplet spreads on the fuel surface as a circle. The instantaneous spreading area can be calculated using the diameter of the circle. Figure 7 shows the calculation process of the spreading area and spreading rate of a single droplet on a fuel surface. The instantaneous diameter of the circle generated by the spreading of the droplet can be obtained using ImageJ, and then the curves of the spreading area and spreading rate over time are obtained using a MATLAB code.

3.3.2 Spreading area of single liquid droplets on liquid fuel surfaces

Figure 8 shows the curves of the spreading area of the foam solutions on the liquid fuel surfaces over time. The FfreeF solution cannot spread on all fuel surfaces, and all the foam solutions used in this study cannot spread on the n-heptane and ethanol surfaces. Thus, the curves of the spreading area of the FfreeF solution on the four liquid fuel surfaces and those of the foam solutions on the n-heptane and ethanol surfaces are not included in Fig. 8.

The spreading phenomenon of all the liquid droplets of foam solutions, except that of FfreeF on the diesel surface, is observed, and the variation of spreading area versus time is illustrated in Fig. 8(A). The spreading area curves increase over time and then remains unchanged after reaching the maximum value. The order of the maximum spreading area is AFFF-5#>AFFF-2#>AFFF-4#>AFFF-6#>AFFF-1#>AFFF-3#, and that of the time required for the liquid droplet to spread completely is AFFF-5#>AFFF-4#>AFFF-6#>AFFF-3#>AFFF-1#>AFFF-2#. The AFFF-5# droplet shows the maximum value of spreading area (639 mm^2) and the shortest spreading time (5.97 s). AFFF-3# has the minimum value of spreading area (21.9 mm^2). The AFFF-2# droplet exhibits the maximum value of the time required to spread completely. The order of the spreading coefficients of foam solution on diesel surface is AFFF-6#>AFFF-4#>AFFF-2#>AFFF-1#>AFFF-5#>AFFF-3#>FfreeF, which is not proportional to the order of the maximum spreading area or the order of the time required for the droplet to spread completely. These results indicate that the spreading coefficient is not the deciding factor of the maximum spreading area.

Figure 8(B) shows the spreading area curves of the foam solutions on the cyclohexane surface. The curves of the AFFF-3# and FfreeF droplets are not included in Fig. 8(B) because these droplets cannot spread on the cyclohexane surface. The spreading area curves of AFFF-5# and AFFF-6# increase gradually over time and remains unchanged after reaching the maximum value. However, the spreading area curves of AFFF-1#, AFFF-2#, and AFFF-4# are almost unchanged over time. The order of the maximum spreading area is AFFF-5#>AFFF-6#>AFFF-2#>AFFF-1#>AFFF-4#. The AFFF-5# droplet still has the maximum value of spreading area of 730.69 mm^2 , which is higher than that on the diesel surface. The maximum spreading area of AFFF-6# is 103.65 mm^2 , which is lower than that on the diesel surface.

3.3.3 Spreading rate of single liquid droplets on liquid fuel surfaces

The instantaneous spreading rate of the foam solution droplets on the liquid fuel surfaces is calculated to analyze the spreading property of the droplets further. The spreading rate is the derivative of spreading area versus time. Figure 9 shows the variation in the spreading rate of the foam solution droplets versus time. For the spreading rate on the diesel surface, AFFF-2#, AFFF-4#, AFFF-5#, and AFFF-6# show a similar change trend, as shown in Fig. 9(A). The spreading rate increases rapidly and then decreases after reaching the maximum value. The spreading rate of AFFF-5# has the maximum value of $247.98 \text{ mm}^2/\text{s}$. The maximum spreading rate values of AFFF-2# ($13.13 \text{ mm}^2/\text{s}$), AFFF-4# ($24.73 \text{ mm}^2/\text{s}$), and AFFF-6# ($18.02 \text{ mm}^2/\text{s}$) are much lower than that of AFFF-5#. However, the spreading rates of AFFF-1# and AFFF-3# show a different variation trend from that of AFFF-2#, AFFF-4#, AFFF-5#, and AFFF-6#. The spreading rate of AFFF-1# decreases rapidly from the beginning, and its maximum value is $23.28 \text{ mm}^2/\text{s}$. The spreading rate of AFFF-3# barely changes over time, and the maximum value is only $1.1 \text{ mm}^2/\text{s}$.

Figure 9(B) shows the variation in the spreading rate of the firefighting foam solution droplets on the cyclohexane surface. The spreading rate of AFFF-5# increases sharply and then decreases sharply after reaching the maximum value of 141.3 mm²/s. The spreading rate curves of AFFF-1#, AFFF-2#, AFFF-4#, and AFFF-6# show a similar change trend, but their maximum spreading rate values are lower than that of AFFF-5#. By contrast, the spreading rates of the firefighting foam solution droplets on the cyclohexane surface are much lower than that on the diesel surface because the foam solutions have a high spreading coefficient on the diesel surface.

Previous studies mainly focused on droplets with low density spreading on surface with high density [38, 39]. The studies on the spreading of droplets with low density spreading on surface with high density are few [40, 41]. The distance of a nonvolatile, immiscible surfactant solution spreading on a deep liquid layer is described by Eq. (2) [38, 39].

$$L(t) = K \frac{S^{1/2}}{(\mu\rho)^{1/4}} t^{3/4} \quad (2)$$

$L(t)$ is spreading distance, t is time, and S is spreading coefficient. μ and ρ represent the viscosity and density of the underlying liquid. Depending on the assumptions imposed on the spreading film, K can range in magnitude from 0.665 to 1.52 [39, 42]. The spreading rate depends on the parameter $S^{1/2}/(\mu\rho)^{1/4}$. However, in this study, the spreading rates of foam solutions are not necessarily related to the parameter $S^{1/2}/(\mu\rho)^{1/4}$. For the same liquid fuel surface, the parameter $\mu\rho$ is fixed and the spreading rate depends on spreading coefficient completely according to the parameter $S^{1/2}/(\mu\rho)^{1/4}$. But, actually, a relative low spreading coefficient of AFFF-5# resulted in the fastest spreading on diesel surface. Joos et al suggested that the reason for the disagreement is that the spreading coefficient S depends on time [40]. Interfaces are expanding during spreading, leading to higher surface and interfacial tensions. For different foam solution formulations, reestablishment of the equilibrium by diffusion associated with demicellization in the bulk is not fast enough as compared with the time scale of expansion [41]. This theory implied that the fastest spreading of AFFF-5# was related to its ability to reach equilibrium surface tension rapidly. Notably, the higher conductivity of AFFF-2#, AFFF-4#, and AFFF-5# showed a faster spreading, implying that an ionic mixture of surfactants has a potential effect on spreading rate [41]. Besides, Svitova et al [35] indicated that the spreading rate depends on the surfactant concentration and the hydrophilicity and hydrocarbon subphase chain length. Considerable works need to be conducted to identify the quantitative relation between these factors and spreading rate in the future.

3.4 Spreading amount of foam solutions on liquid fuel surfaces

Single liquid droplets of several AFFF solutions can spread on diesel or cyclohexane surfaces. However, the AFFF solutions have higher density compared with liquid fuel. When foam solution droplets are continuously released onto liquid fuel surfaces, the droplets must escape from the fuel surface and sink to the bottom once the accumulated amount of foam solution on the fuel surface reaches a certain value. During the accumulation of droplets on the liquid fuel surface, the accumulated volume of foam solution on the liquid fuel surface is characterized as the spreading amount when the first droplet under the liquid fuel surface escapes from liquid fuel surface and begins to sink. In the spreading amount experiments, the syringe pump used is adjusted to generate a 0.01 ml droplet, and the generation rate is fixed, 0.35 ml/min. The number of droplets released to the fuel surface is recorded as the spreading amount when a droplet escapes from the liquid fuel surface and begins to sink.

Taking the case of the AFFF-5# solution on the diesel surface as an example, Fig. 10 shows the quantitative description of spread amount of AFFF-5# droplets on diesel surface. At 45240 ms, the 26th droplet of AFFF-5# impacted diesel surface, and then the first droplet under the liquid fuel surface escaped from liquid fuel surface and sinks to the bottom at 46000 ms. 25 droplets (0.25 ml) accumulated on the diesel surface before the first droplet sinks. Thus, the spread amount of AFFF-5# on diesel surface is 25 droplets, 0.25 ml.

Figure 11 shows the spreading amount of the AFFF solutions on the liquid fuel surfaces. All the AFFF solutions can spread on the diesel surface, but a significant difference exists in spreading amount, as shown in Fig. 11 (A). AFFF-5# shows the largest spreading amount of 0.25 ml even if its spreading coefficient on the diesel surface is lower than that of AFFF-1#, AFFF-2#,

AFFF-4#, and AFFF-6#. AFFF-1# and AFFF-3# have the same spreading amount of 0.04 ml, and AFFF-2# and AFFF-6# have the same spreading amount of 0.06 ml. Interestingly, the spreading amount of AFFF-4# is only 0.05 ml, which is lower than that of AFFF-2# and AFFF-6#, even though it has a higher maximum spreading area and spreading rate. These results indicated that the spreading amount is not proportional to the spreading coefficient. That is, a large spreading coefficient or high spreading rate does not necessarily lead to a large spreading amount. The spreading amount is affected by many factors in addition to surface and interfacial tension. Such factors include the viscosity of foam solutions, surface wettability, wetting angle, density of foam solution and fuel [36].

The spreading amount of the AFFF solutions on the cyclohexane surface is apparently different from that on the diesel surface, as shown in Fig. 11(B). The spreading amount of all the foam solutions on the cyclohexane surface is lower than that on the diesel surface. AFFF-5# keeps the maximum value of spreading amount on the cyclohexane surface. The spreading amount of AFFF-3# on the cyclohexane surface is zero, which is similar to that of FfreeF. These results suggest that the spreading amount is significantly affected by the type of liquid fuel surface and firefighting foam formulations. For the different fuel surface, a higher spreading coefficient resulted in a greater spreading amount. For the same liquid fuel surface, the spread amount is not necessarily associated with the equilibrium spreading coefficient. The difference of spreading amount between the firefighting foam solutions is probably affected by the dynamic spreading coefficient, viscosity, conductivity and type of surfactants.

4. Conclusion

A series of experiments on the spreading behavior of firefighting foam solution droplets on typical liquid fuel surfaces is conducted. The spreading coefficient, spreading behavior, spreading area, spreading rate, and spreading amount are analyzed systematically. The following conclusions can be drawn from this work:

The spreading coefficients of all the AFFF and fluorine-free foam solutions used in this study on the diesel and cyclohexane surfaces are positive, whereas those of the AFFF-3#, AFFF-5#, and FfreeF solutions on the n-heptane surface are negative.

Four spreading phenomena, namely, spreading, suspension, dissolution, and sinking, of AFFF solutions on liquid fuel surfaces are identified. For foam solutions with a negative spreading coefficient, no spreading occurs on the liquid fuel surface; however, a positive spreading coefficient does not necessarily lead to the formation of an aqueous film.

Generally, a high spreading coefficient leads to a good spreading area, spreading rate, and spreading amount; however, none of the spreading area, spreading rate, and spreading amount is proportional to the spreading coefficient. Many factors affect spreading property, including dynamic spreading coefficient, viscosity and density of liquid fuel, type and concentrations of surfactants, and so on. Quantitative studies on these factors must be conducted in next works.

A significant difference exists in the spreading properties of commercially fluorinated and fluorine-free foams on the liquid fuel surfaces used in this study. During the evaluation of the performance of firefighting foams, the spreading property, spreading coefficient, spreading rate, and spreading amount must be focused on instead of only the spreading coefficient.

Declarations

Acknowledgment

The present work was supported by the National Natural Science Foundation of China (No. 51904230), and Natural Science Basic Research Program of Shaanxi (No. 2020JQ-755).

References

1. Zhao, J., Chen, S. & Liu, Y. Dynamical behaviors of droplet impingement and spreading on chemically heterogeneous surfaces. *Appl. Surf. Sci.* **400**, 515–523 (2017).

2. Liang, G., Guo, Y., Mu, X. & Shen, S. Experimental investigation of a drop impacting on wetted spheres. *Exp. Therm. Fluid Sci.* **55**, 150–157 (2014).
3. Liang, G. *et al.* Crown behavior and bubble entrainment during a drop impact on a liquid film. *Theor. Comput. Fluid Dyn.* **28** (2), 159–170 (2013).
4. Šikalo, A., Marengo, M., Tropea, C. & Ganic, E. N. Analysis of impact of droplet on horizontal surface. *Exp. Therm. Fluid Sci.* **25**, 503–510 (2002).
5. Liang, G. & Mudawar, I. Review of mass and momentum interactions during drop impact on a liquid film. *Int. J. Heat Mass Transf.* **101**, 577–599 (2016).
6. Xu, M., Wang, C. & Lu, S. Water droplet impacting on burning or unburned liquid pool. *Exp. Therm. Fluid Sci.* **85**, 313–321 (2017).
7. Zou, J., Ren, Y. L., Ji, C., Ruan, X. D. & Fu, X. Phenomena of a drop impact on a restricted liquid surface. *Exp. Therm. Fluid Sci.* **51**, 332–341 (2013).
8. Zou, J., Wang, P. F., Zhang, T. R., Fu, X. & Ruan, X. Experimental study of a drop bouncing on a liquid surface. *Phys. Fluids.* **23** (4), 044101 (2011).
9. Rodriguez, F. & Mesler, R. Some drops don't splash. *J. Colloid Interface Sci.* **106**, 347–352 (1985).
10. Choudhury, R., Choi, J., Yang, S., Kim, Y. J. & Lee, D. Maximum spreading of liquid drop on various substrates with different wettabilities. *Appl. Surf. Sci.* **415**, 149–154 (2017).
11. Manzello, S. L. & Yang, J. C. An experimental study of a droplet impinging on a liquid surface. *Exp. Fluids.* **32**, 580–589 (2002).
12. Sikalo, S. & Ganic, E. N. Phenomena of droplet–surface interaction. *Exp. Therm. Fluid Sci.* **31**, 97–110 (2006).
13. Yao, Y., Li, C., Zhang, H. & Yang, R. Modelling the impact, spreading and freezing of a water droplet on horizontal and inclined superhydrophobic cooled surfaces. *Appl. Surf. Sci.* **419**, 52–62 (2017).
14. Woodman, A. L., Richter, H. P., Adicoff, A. & Gordon, A. S. AFFF spreading properties at elevated temperatures. *Fire Technol.* **14**, 265–272 (1978).
15. Sheinson, R. S. *et al.* The future of aqueous film forming foam (AFFF): performance parameters and requirements. National Institute of Standards and Technology (US Dept of Commerce), 2002.
16. Sheng, Y., Jiang, N., Sun, X. & Lu, S. C. Li Experimental study on effect of foam stabilizers on aqueous film-forming foam. *Fire Technol.* **54** (1), 211–228 (2018).
17. Sheng, Y., Jiang, N., Lu, S. & Li, C. Fluorinated and fluorine-free firefighting foams spread on heptane surface. *Colloid Surface A.* **552**, 1–8 (2018).
18. Moran, H. E., Burnett, J. C. & Leonard, J. T. Suppression of Fuel Evaporation by Aqueous Films of Fluorochemical Surfactant Solutions (No.NRL-7247). Naval Research Lab Washington DC, 1971.
19. Williams, B. *et al.* Extinguishment and Burnback tests of fluorinated and fluorine-free firefighting foams with and without film formation. suppression, detection, and signaling research and applications (SUPDET), 2011.
20. Jia, X. *et al.* Two–dimensional spreading properties and sealing characteristics of fluorocarbon surfactants on several typical hydrocarbon fuels. *Sci Rep-UK.* **11**, 1148 (2021).
21. BS EN 1568-3-2008: Fire extinguishing mediFfreeF concentrates-Part 3: specification for low expansion foam concentrates for surface application to water-immiscible liquids
22. DEF(AUST)5706 (2003) Foam, liquid fire extinguishing; 3 percent and 6 percent concentrate specification, Commonwealth of Australia, Australian Defence Standard
23. Lattimer, B. Y., Hanauska, C. P. & Scheffey, J. L. F.W. Williams The use of small-scale test data to characterize some aspects of firefighting foam for suppression modeling. *Fire Saf J.* **38**, 117–146 (2003).
24. Magrabi, S. A., Dlugogorski, B. Z. & Jameson, G. J. Free drainage in aqueous foams: model and experimental study. *AIChE J.* **47**, 314–327 (2001).

25. Magrabi, S. A., Dlugogorski, B. Z. & Jameson, G. J. A comparative study of drainage characteristics in AFFF and FFFP compressed-air firefighting foams. *Fire Saf J.* **37**, 21–51 (2002).
26. Sheng, Y., Lu, S., Xu, M., Wu, X. & Li, C. Effect of Xanthan gum on the performance of aqueous film-forming foam. *J. Dispers. Sci. Technol.* **37**, 1664–1670 (2016).
27. Zhang, Q. *et al.* Experimental investigation of foam spread and extinguishment of the large-scale methanol pool fire. *J Hazard Mater.* **287**, 87–92 (2015).
28. Laundess, A. J., Rayson, M. S., Kennedy, E. M. & Dlugogorski, B. Z. Small-scale test protocol for firefighting foams DEF (AUST) 5706: effect of bubble size distribution and ER. *Fire Technol.* **47**, 149–162 (2011).
29. Sheng, Y., Jiang, N., Lu, S., Wang, Q. & Zhao, Y. X. Liu. Study of Environmental-Friendly Firefighting Foam Based on the Mixture of Hydrocarbon and Silicone Surfactants. *Fire Technol.* (2019) 1–17.
30. Hetzer, R., Kümmerlen, F., Wirz, K. & Blunk, D. Fire testing a new fluorine-free affff based on a novel class of environmentally sound high performance siloxane surfactants. *Fire Safety Science.* **11**, 1261–1270 (2014).
31. Eastoe, J. & Dalton, J. S. Dynamic surface tension and adsorption mechanisms of surfactants at the air–water interface. *Adv. Colloid Interface Sci.* **85** (2–3), 103–144 (2000).
32. Liang, G. T., Guo, Y., Yang, Y., Guo, S. & Shen, S. Q. Special phenomena from a single liquid drop impact on wetted cylindrical. *Exp. Therm. Fluid Sci.* **51**, 18–27 (2013).
33. Kang, Q. S., Lu, S. X. & Chen, B. Experimental study on burning rate of small scale heptane pool fires. *Chin. Sci. Bulletin.* **55**, 973–979 (2009).
34. Flick, E. W. *Industrial Solvents Handbook* third edn (Noyes Publications, Park Ridge, 1985).
35. Svitova, T., Hoffmann, H. & Hill, R. M. Trisiloxane surfactants: surface/interfacial tension dynamics and spreading on hydrophobic surfaces. *Langmuir.* **12** (7), 1712–1721 (1996).
36. Myers, D. *Surfaces, Interfaces, and Colloids—Principles and Applications.* New York: Wiley-VCH, second edition, 1999.
37. Phan, C. M., Allen, B., Peters, L. B., Le, T. N. & Tade, M. O. *Can water float on oil?* *Langmuir.* **28** (10), 4609–4613 (2012).
38. Fay, J. A. The spread of oil slicks on a calm sea in *Oil on the Sea*, edited by D. Hoult ~ Plenum, New York 1969.
39. Dussaud, A. D. & Troian, S. M. Dynamics of spontaneous spreading with evaporation on a deep fluid layer. *Phys. Fluids.* **10** (1), 23–38 (1998).
40. Joos, P. & Van Hunsel, J. Spreading of aqueous surfactant solutions on organic liquids. *J. Colloid Interface Sci.* **106** (1), 161–167 (1985).
41. Rillaerts, E. & Joos, P. Rate of demicellization from the dynamic surface tensions of micellar solutions. *The Journal of Physical Chemistry.* **86** (17), 3471–3478 (1982).
42. Camp, D. W. Ph.D. thesis, University of Washington, Dept. of Chem. Eng 1985.

Figures

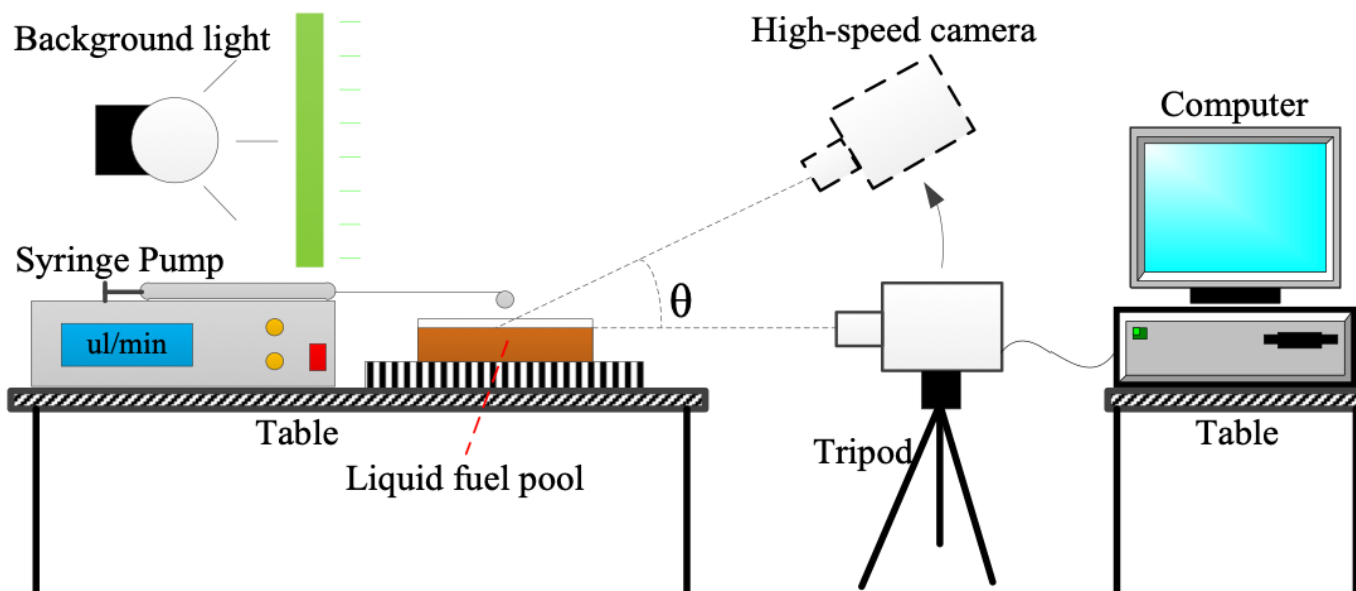


Figure 1

Schematic of apparatus for spread dynamic of foam solution on liquid fuel surface.

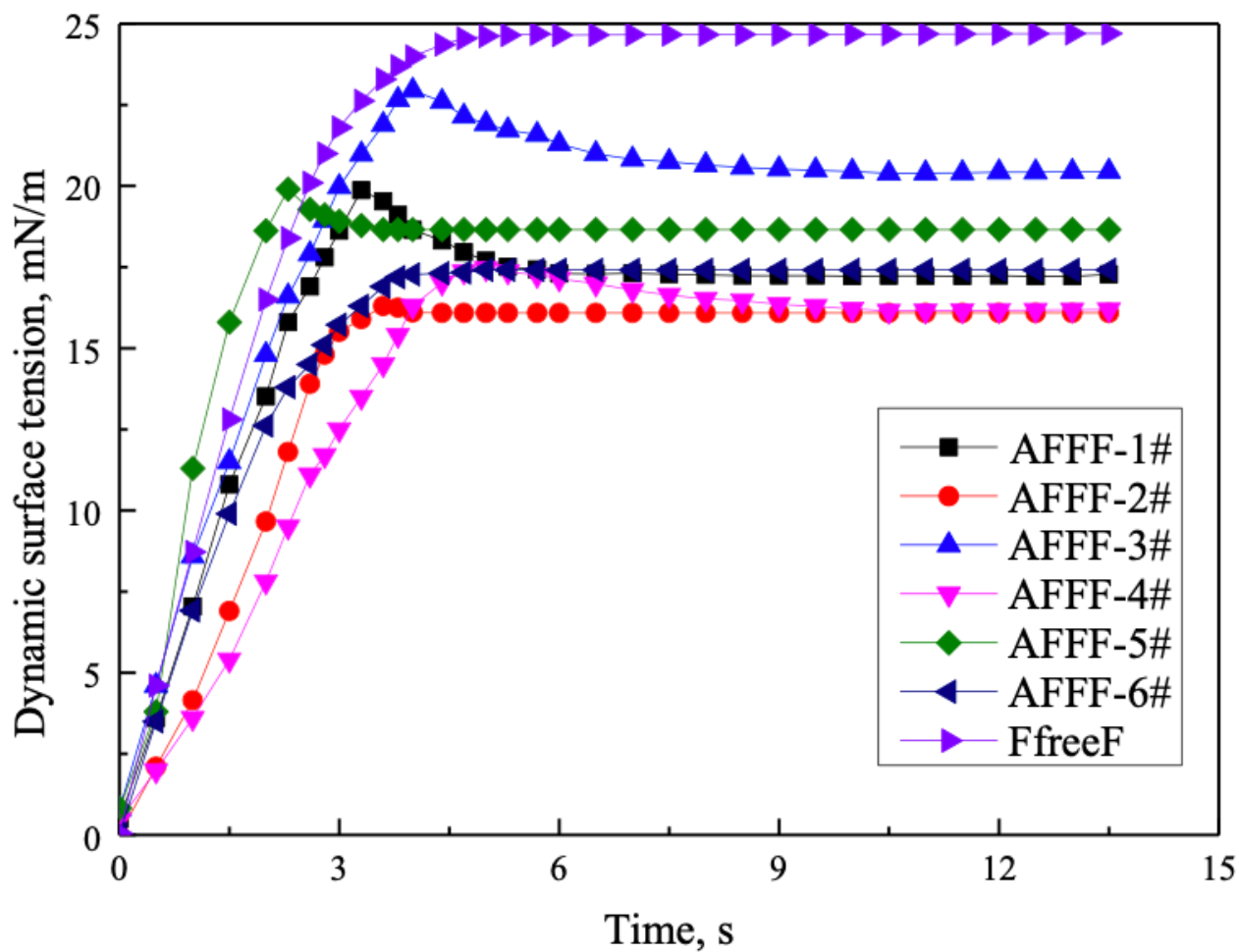


Figure 2

Variation in the dynamic surface tension of the seven firefighting foam solutions versus time.

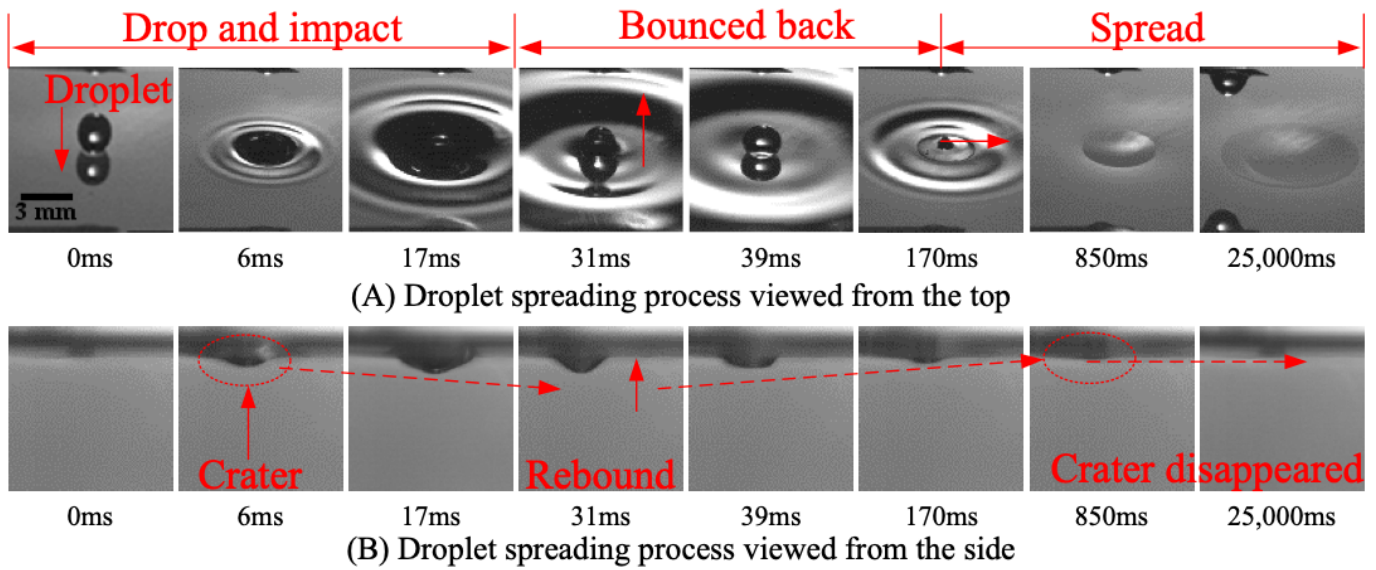


Figure 3

Spread process of single droplet of foam solution on liquid fuel surface.

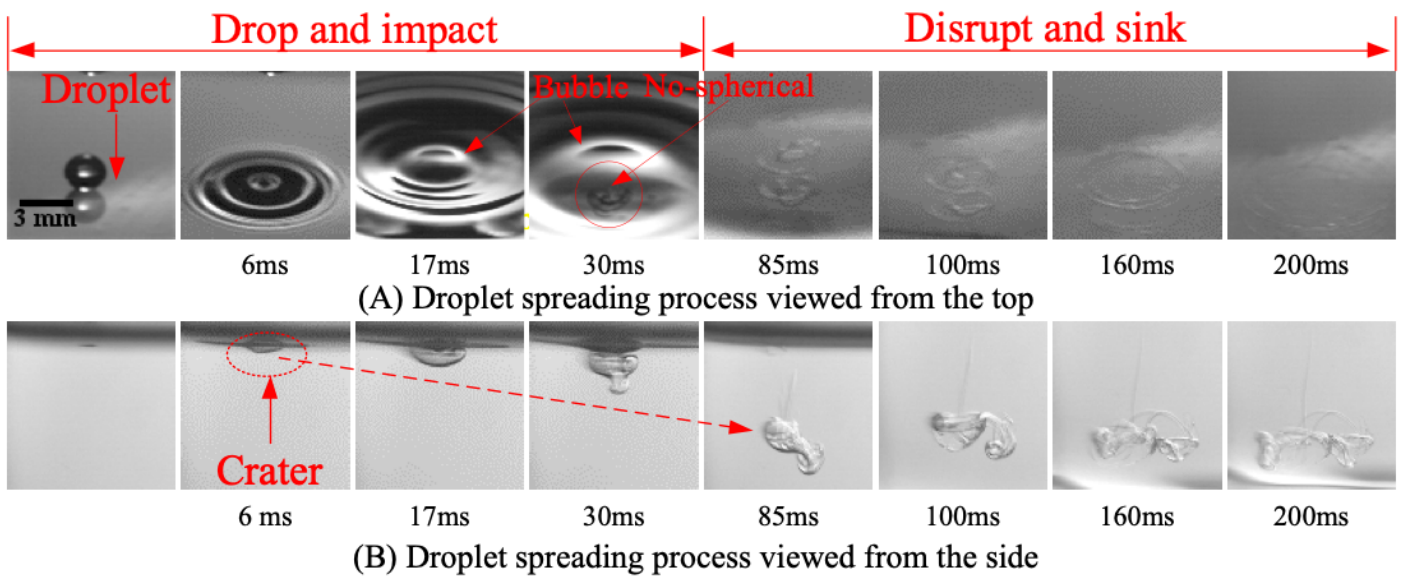


Figure 4

The spreading process of AFFF-1# on the ethanol surface.

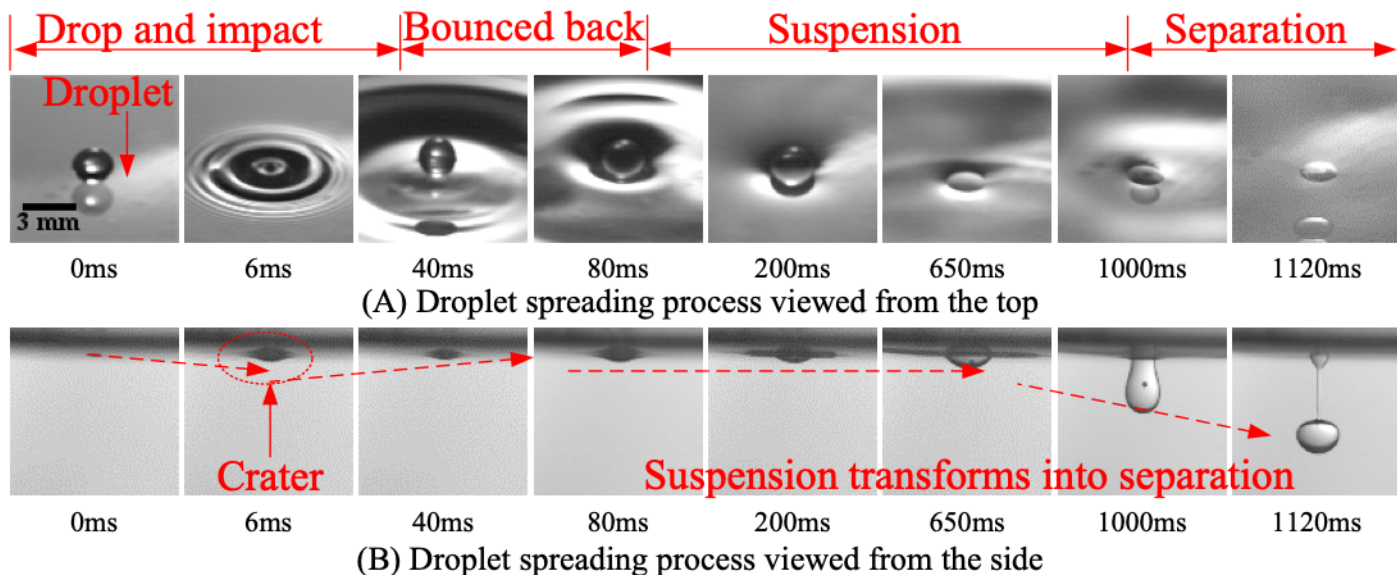


Figure 5

The spreading process of the AFFF-1# droplet on the heptane surface.

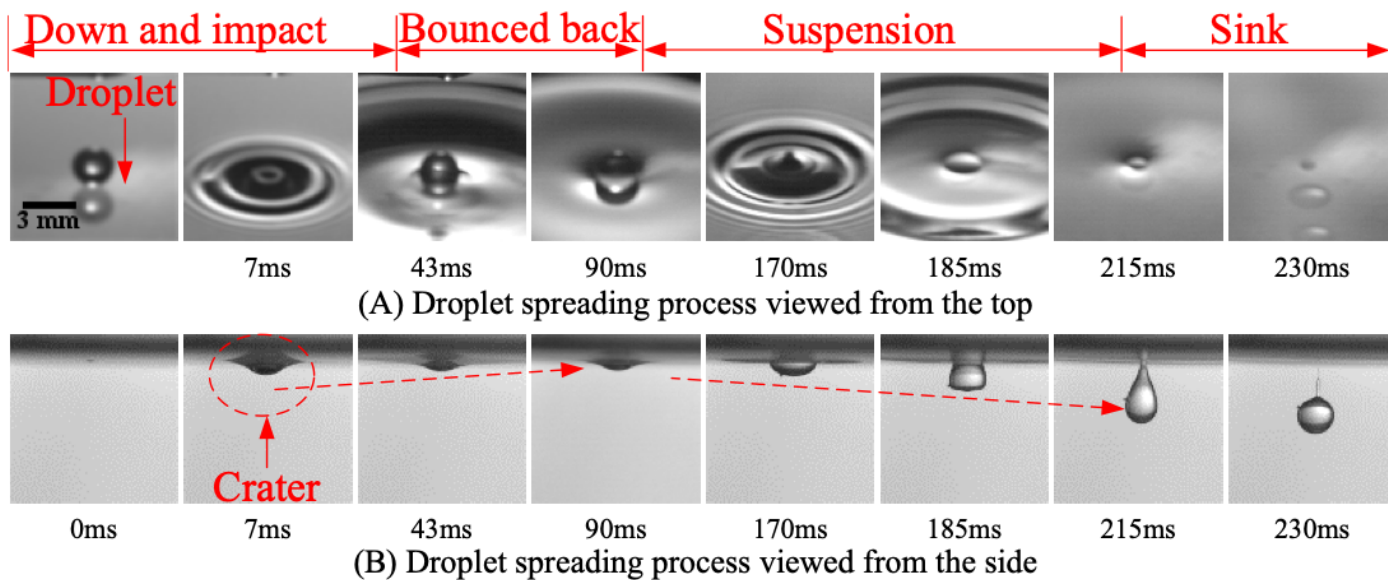


Figure 6

The spreading process of AFFF-3# on cyclohexane surface.

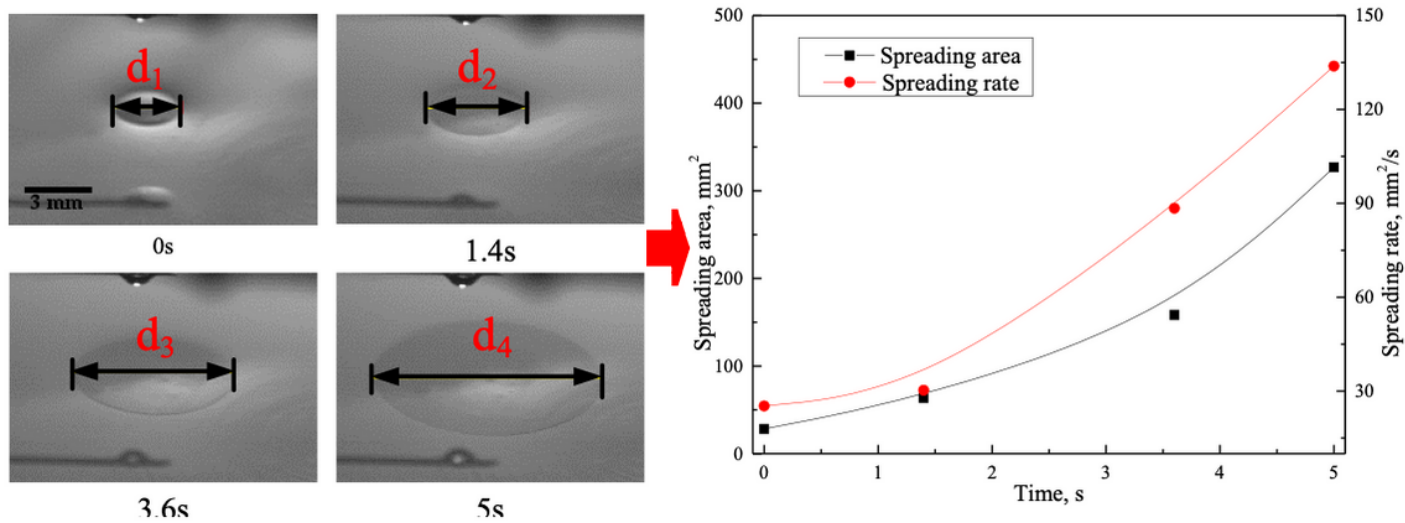


Figure 7

Quantitative description of spread process of single liquid droplet on surface of typical liquid fuel. (AFFF-5# spread on cyclohexane surface).

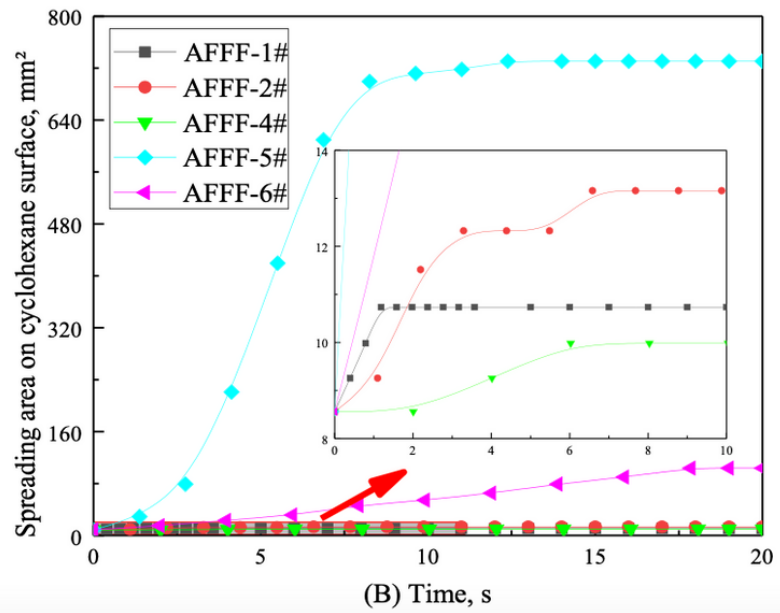
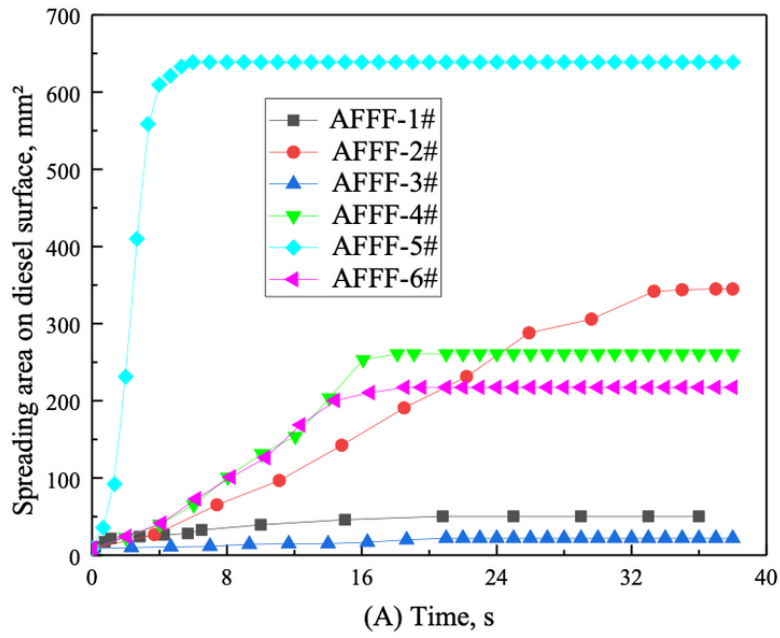


Figure 8

Variation in spread area of single liquid droplet of firefighting foam solution on liquid fuel surface.

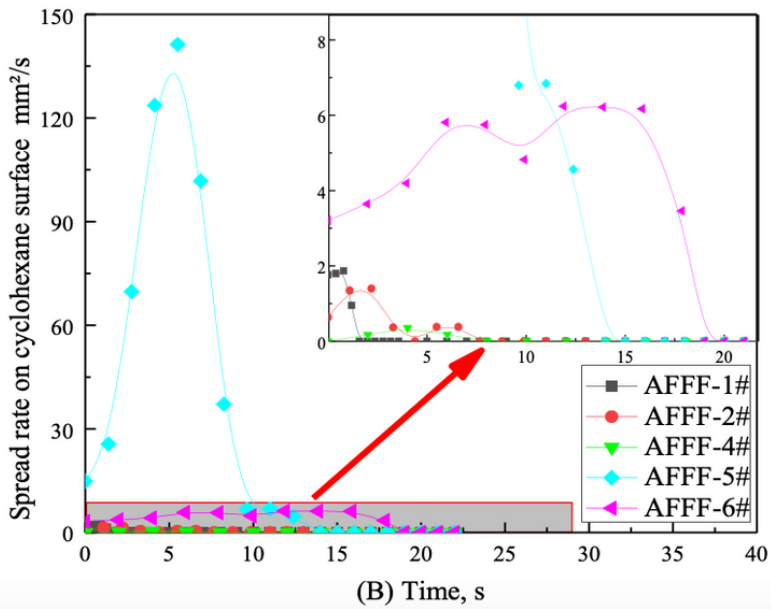
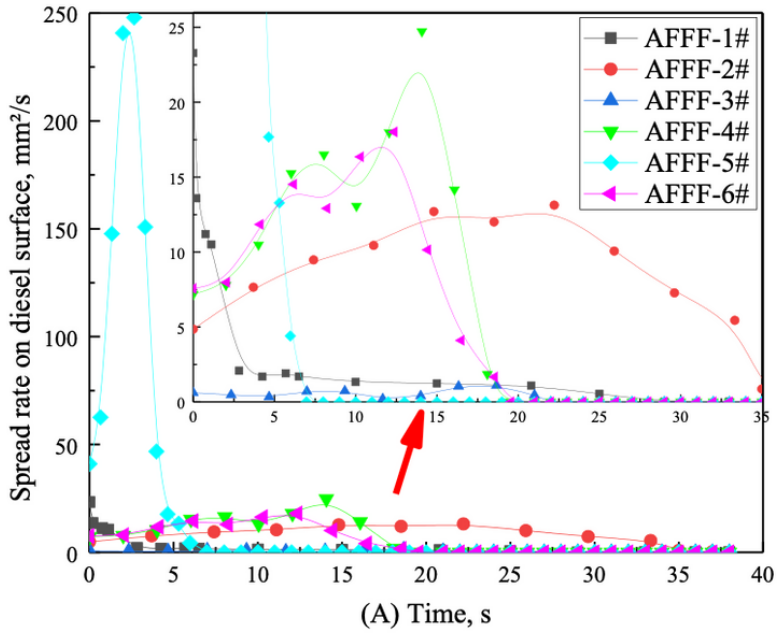


Figure 9

Variation in spread rate of single liquid droplet of firefighting foam solution on diesel surface and cyclohexane surface.

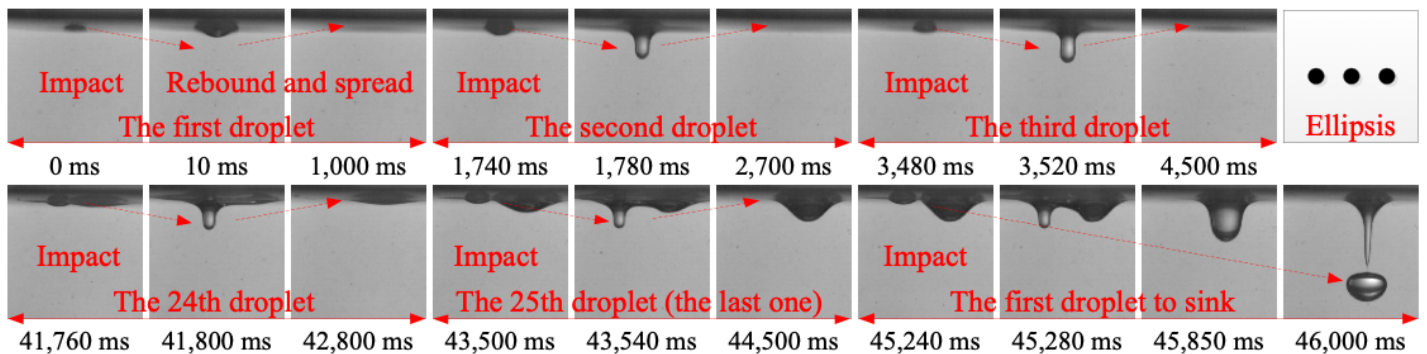
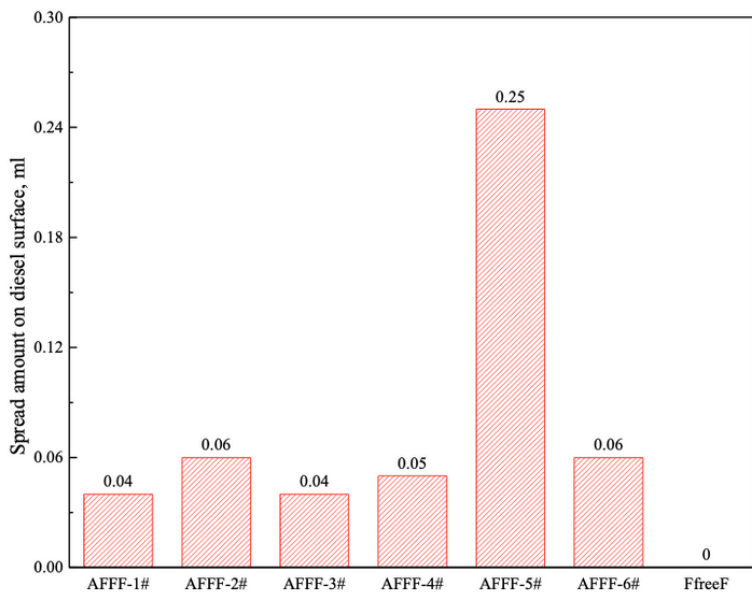
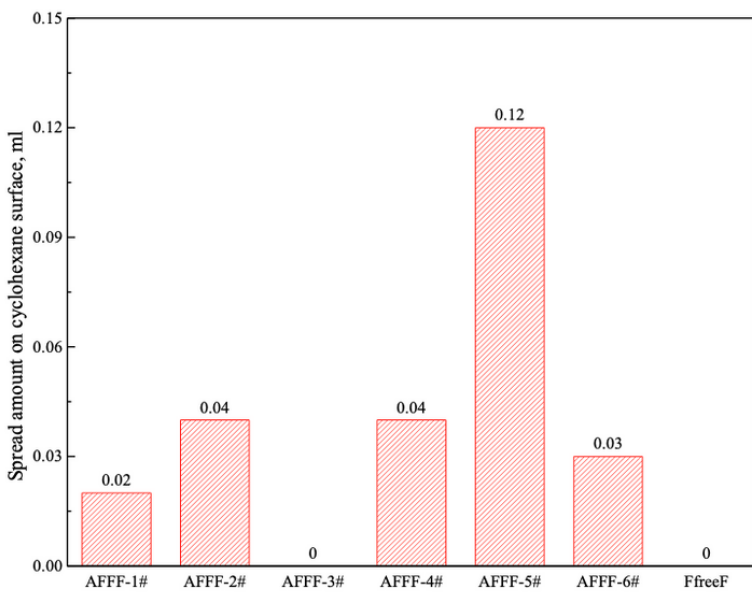


Figure 10

Quantitative description of spread amount of AFFF-5# droplets on diesel surface.



(A) Firefighting foams



(B) Firefighting foams

Figure 11

Spread amount of firefighting foam solution on diesel and cyclohexane surfaces.